Picosecond Dynamics of Photoinduced Interligand Electron Transfer in $[Re(MQ^+)(CO)_3(dmb)]^{2+}$ (dmb = 4,4′-Dimethyl-2,2′-bipyridine, MQ^+ = *N*-Methyl-4,4′-bipyridinium)

Davina J. Liard and Antonín Vlček, Jr.*

Department of Chemistry, Queen Mary and Westfield College, University of London, London E1 4NS, United Kingdom

Received June 30, 1999

Excited-state dynamics of $[Re(MQ^+)(CO)_3(dmb)]^{2+}$, (dmb = 4,4′-dimethyl-2,2′-bipyridine, MQ^+ = *N*-methyl-4,4′-bipyridinium) was studied by femtosecond time-resolved spectroscopy in the visible spectral region. Excitation at 400 or 330 nm prepares a mixture of Re → dmb and Re → MQ^+ metal-to-ligand charge-transfer, MLCT, states. The Re → dmb MLCT state undergoes a $dmb^{\bullet-}$ → MQ^+ interligand electron transfer to produce a relatively long-lived Re → MQ^+ MLCT excited state, which was characterized spectroscopically. The lifetime of this reaction was determined as 8.3 ps in CH_3CN. The interligand electron transfer occurs as a nonadiabatic process in the Marcus normal region. The electronic coupling was estimated to lie in the range 20−40 cm^{-1}. The electron transfer becomes partially adiabatic in ethylene glycol solutions for which the reaction lifetime of 14.0 ps was determined. Depending on the medium relaxation time, the principal control of the electron-transfer rate changes from electron tunneling to solvent relaxation.

Introduction

Photoinduced electron transfer between a chromophore and a covalently linked electron acceptor or donor represents a convenient way to create an intramolecular separation of oxidizing and reducing sites by optical excitation. If long-lived enough, such charge-separated states can be utilized in followup redox processes. Ultimately, the optical energy or information carried by the incident light is converted and/or stored by chemical means. To function efficiently, the charge separation must develop very rapidly, preferentially on a femtosecond or picosecond time scale. Besides their potential utility in light energy conversion or molecular photonic devices, ultrafast excited-state electron-transfer reactions often display new and/or poorly understood phenomena, for example, rates comparable with vibrational or solvent dynamics, conformational gating, or transition between adiabatic and nonadiabatic behavior.[1−3]

With these motivations, we have embarked on studies of interligand, possibly ultrafast, electron transfer in organometallic complexes which contain two different electron acceptor ligands. Metal-to-ligand charge transfer, MLCT, excitation of such species can trigger an ultrafast electron transfer from one ligand to another:

$$M(A)(L) \xrightarrow{h\nu} M^+(A)(L^{\bullet-}) \xrightarrow{et} M^+(A^{\bullet-})(L)$$

Such an interligand electron transfer is equivalent to a nonradiative transition between two MLCT excited states, making a conceptual link between electron-transfer reactions and excited-state dynamics. In principle, the kinetics and mechanism of this process can be controlled by the electronic coupling between the redox sites $L^{\bullet-}$ and A through the metal atom, by vibrational relaxation of the two MLCT excited states involved, solvent dynamics, and/or the conformational dynamics of the acceptor ligand A. In the case of a strong electronic coupling, electron transfer can occur in the adiabatic regime or at the adiabatic/nonadiabatic boundary, depending on the solvent.

Herein, we report results of an ultrafast spectroscopic study of the complex[4−8] $[Re(MQ^+)(CO)_3(dmb)]^{2+}$ (dmb = 4,4′-dimethyl-2,2′-bipyridine, MQ^+ = *N*-methyl-4,4′-bipyridinium) whose schematic structure is shown in Scheme 1. The MQ^+ electron acceptor is directly coordinated to a robust $Re(CO)_3(dmb)^+$ chromophore, which undergoes a Re → dmb MLCT excitation on irradiation. However, fluid solutions of $[Re(MQ^+)(CO)_3(dmb)]^{2+}$ do not show the typical MLCT emission, and the Re → MQ^+ MLCT excited state, $[Re^{II}(MQ^{\bullet})(CO)_3(dmb)]^{2+}$, is the only species which was detected and characterized on a nanosecond time scale by time-resolved UV−vis absorption[5] and resonance Raman spectroscopy.[7] Hence, it was concluded[4−7] that the optically prepared Re → dmb MLCT excited state $[Re^{II}(MQ^+)(CO)_3(dmb^{\bullet-})]^{2+}$ undergoes a fast interligand $dmb^{\bullet-}$ → MQ^+ electron transfer whose nature and rate remained, however, obscure. To observe this process directly and unravel its nature, dynamics, and mechanism, we have prepared the initial Re → dmb MLCT excited state by irradiating $[Re(MQ^+)(CO)_3(dmb)]^{2+}$ with 250 fs laser pulses and followed the ensuing dynamics by time-resolved absorption spectroscopy in the visible spectral region. Two solvents with vastly different relaxation

(1) Ratner, M. A.; Jortner, J. In *Molecular Electronics*; Jortner, J., Ratner, M., Eds.; Blackwell Science Ltd.: Oxford, 1997; p 5.
(2) Balzani, V.; Scandola, F. *Supramolecular Photochemistry*; Ellis Horwood: Chichester, 1991.
(3) Barbara, P. F.; Meyer, T. J.; Ratner, M. A. *J. Phys. Chem.* **1996**, *100*, 13148.
(4) Westmoreland, T. D.; Le Bozec, H.; Murray, R. W.; Meyer, T. J. *J. Am. Chem. Soc.* **1983**, *105*, 5952.
(5) Chen, P.; Danielson, E.; Meyer, T. J. *J. Phys. Chem.* **1988**, *92*, 3708.
(6) Chen, P.; Curry, M.; Meyer, T. J. *Inorg. Chem.* **1989**, *28*, 2271.
(7) Schoonover, J. R.; Chen, P.; Bates, W. D.; Dyer, R. B.; Meyer, T. J. *Inorg. Chem.* **1994**, *33*, 793.
(8) Mecklenburg, S. L.; Opperman, K. A.; Chen, P.; Meyer, T. J. *J. Phys. Chem.* **1996**, *100*, 15145.

10.1021/ic990770f CCC: $19.00
Published on Web 01/20/2000

Scheme 1. Photoinduced Interligand Electron Transfer in $[Re(MQ^+)(Co)_3(dmb)]^{2+}$ and Schematic Structures of the Species Involved

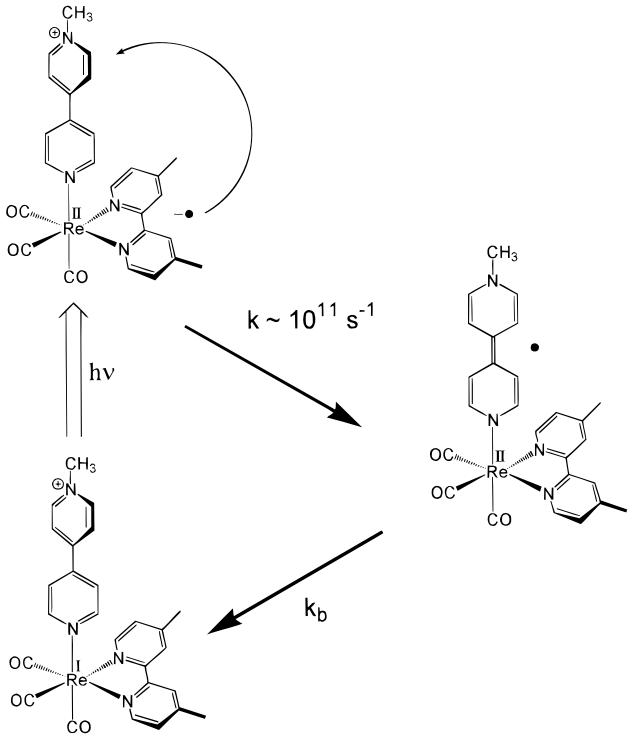

times, acetonitrile and ethylene glycol, were used to explore possible adiabatic effects.

Experimental Section

Acetonitrile and ethylene glycol of spectroscopic quality were supplied by Aldrich. Cyclic voltammetry was measured using a potentiostat model 263A, EG&G Instruments. The MQ^+ ligand[9,10] and the $[Re(MQ^+)(CO)_3(dmb)](PF_6)_2$ complex[8] were prepared by a published procedure and characterized by IR, UV−vis, and ^1H and ^{13}C NMR spectroscopy. Data for $[Re(MQ^+)(CO)_3(dmb)](PF_6)_2$: IR ($CH_3CN$) ν_{max} 2036(s), 1932(br) cm^{-1}; ^1H NMR δ_H (CD_2Cl_2) 2.60 (6H, s, Me-dmb), 4.40 (3H, s, Me-MQ^+), 7.55 (2H, d, $J = 5.8$ Hz, dmb), 7.68 (2H, dd, $J = 5.2$, 1.6 Hz, MQ^+), 8.08 (2H, s, dmb), 8.17 (2H, d, $J = 7.1$ Hz, MQ^+), 8.33 (2H, $J = 5.3$, 1.5 Hz, MQ^+), 8.64 (2H, d, $J = 6.9$ Hz, MQ^+), 8.94 (2H, d, $J = 5.8$ Hz, dmb); ^{13}C NMR δ_C (CD_3CN) 20.62 (Me-dmb), 48.25 (Me-MQ^+), 191.84 (CO axial), 195.634(CO equatorial). Data for $[Re(4\text{-}Etpy)(CO)_3(dmb)](PF_6)_2$: IR ($CH_3CN$) ν_{max} 2034(s), 1930(br) cm^{-1}; ^1H NMR δ_H (benzene-d_6) 0.67 (3H, t, $J = 7.6$ Hz, CH_3-Etpy), 1.91 (2H, q, $J = 7.6$ Hz, CH_2-Etpy), 2.08 (6H, s, Me-dmb), 6.34 (2H, dd, $J = 4.9$ Hz, Etpy), 6.72 (2H, d, $J = 6.4$ Hz, dmb), 7.71 (2H, d, $J = 6.5$ Hz, Etpy), 8.04 (2H, s, dmb), 8.11 (2H, d, $J = 5.6$ Hz, dmb); ^{13}C NMR δ_C (CD_3CN) 12.96 (CH_3-Etpy), 20.68 (Me-dmb), 27.57 (CH_2-Etpy), 195.85 (CO equatorial), CO axial not seen.

Ultrafast spectroscopic experiments were carried out on flowing, degassed solutions whose absorbance at the excitation wavelength was kept in the range 0.6−1.0. The solutions were photostable, and no sample photodecomposition occurred during measurements. The time-resolved spectroscopy setup has been described elsewhere.[11−15] The sample was excited using the 400 nm second harmonic of a Spectra Physics Tsunami titanium−sapphire regenerative amplifier operating at a repetition rate of ~1 kHz and producing pulses of approximately 250 fs duration (fwhm). A pulse energy of 1 μJ was used. Alternatively, the excitation at 330 nm (0.1 μJ) employed a frequency-doubled 660 nm output of an optical parametric amplifier pumped by the 800 nm Ti:sapphire fundamental. The white light continuum probe beam was generated by passing the Ti:sapphire fundamental through a cell with D_2O. The delay between the excitation and probe pulses was controlled by an optical delay line. Diode array detection involved dividing the probe pulse into two parts and sending one part through the sample before dispersing it onto a 512 pixel diode array and dispersing the other part directly onto a reference diode array, bypassing the sample. The excitation pulse was blocked every alternative laser pulse using a mechanical chopper. Data were collected from these diode arrays over 20 s for each time delay. The measurements at individual delay times were repeated 10 times in a random order. The data were processed to give difference absorption spectra (i.e., the spectrum after excitation minus the spectrum before excitation). Kinetic profiles at a single wavelength were measured using probe pulses obtained by selecting a portion of the white light continuum with a 10 nm band-pass interference filter. The excitation beam was chopped mechanically at a frequency of ca. 200 Hz. Intensities of the sample and reference probe beams were monitored using two photodiodes. An analogue ratio of the photodiode signals was obtained and fed into a lock-in amplifier. Signals were accumulated at each delay time for 5 s, and the whole measurement was repeated at least 10 times, again in a random order of the delay times. The data were processed to give the difference between the sample absorbance measured with and without the laser excitation (Δ(absorbance)) as a function of the delay time. Fitting of the experimental kinetics was performed with Microcal Origin version 5.0 software.

Results and Discussion

Absorption Spectra and Electrochemistry. Electronic absorption spectra of $[Re(MQ^+)(CO)_3(dmb)]^{2+}$ in CH_3CN or ethylene glycol solutions show a broad, intense absorption band at 337 nm, $\epsilon = 1.10 \times 10^4\ M^{-1}\ cm^{-1}$ in CH_3CN or $1.02 \times 10^4\ M^{-1}\ cm^{-1}$ in ethylene glycol. The position, intensity, and a small solvatochromism of this absorption band, manifested by a red shift on going to the less polar 1,2-dichloroethane solvent ($\lambda_{max} = 349$ nm), are characteristic of its MLCT character. The $[Re(Etpy)(CO)_3(dmb)]^+$ complex, in which the electron acceptor MQ^+ is replaced by an innocent 4-ethylpyridine ligand, displays a similar absorption band at 339 nm in CH_3CN, but of a lower intensity, $\epsilon = 5.70 \times 10^3\ M^{-1}\ cm^{-1}$. This band corresponds to the Re → dmb MLCT transition. The spectra of $[Re(MQ^+)(CO)_3(dmb)]^{2+}$ and $[Re(Etpy)(CO)_3(dmb)]^+$, obtained in CH_3CN solutions, are displayed in Figure 1. The difference in the intensities of the MLCT absorption bands of these two complexes indicates that the 337 nm band of $[Re(MQ^+)(CO)_3(dmb)]^{2+}$ is actually a superposition of two bands, due to Re → dmb and Re → MQ^+ MLCT transitions which have approximately equal intensities; see the Figure 1 caption. This is in accordance with resonance Raman spectra of $[Re(MQ^+)(CO)_3(bpy)]^{2+}$ measured using 363.8 or 406.7 nm excitation, which showed resonantly enhanced peaks due to both bpy and MQ^+ vibrations.[7]

Electrochemical reduction of $[Re(MQ^+)(CO)_3(dmb)]^{2+}$ was investigated by cyclic voltammetry in both CH_3CN and ethylene glycol at 273 K using a glassy carbon electrode and 0.1 M $LiClO_4$ as a supporting electrolyte at a 200 mV/s scan rate. Two fully reversible reduction waves at $E_{1/2} = -1.30$ and -1.79 V

(9) Seiler, M.; Durr, H. *Synthesis* **1994**, 83.
(10) Coe, B. J.; Chamberlain, M. C.; Essex-Lopresti, J. P.; Gaines, S.; Jeffery, J. C.; Houbrechts, S.; Persoons, A. *Inorg. Chem.* **1997**, *36*, 3284.
(11) Farrell, I. R.; Matousek, P.; Vlček, A., Jr. *J. Am. Chem. Soc.* **1999**, *121*, 5296.
(12) Farrell, I. R.; Matousek, P.; Kleverlaan, C. J.; Vlček, A., Jr. *Chem.-Eur. J.*, in press.
(13) Matousek, P.; Parker, A. W.; Taday, P. F.; Toner, W. T.; Towrie, M. *Opt. Commun.* **1996**, *127*, 307.
(14) Towrie, M.; Parker, A. W.; Shaikh, W.; Matousek, P. *Meas. Sci. Technol.* **1998**, *9*, 816.
(15) Towrie, M.; Matousek, P.; Parker, A. W.; Jackson, S.; Bisby, R. H. *Rutherford Appleton Lab. Rep.* **1997/1998**, 183.

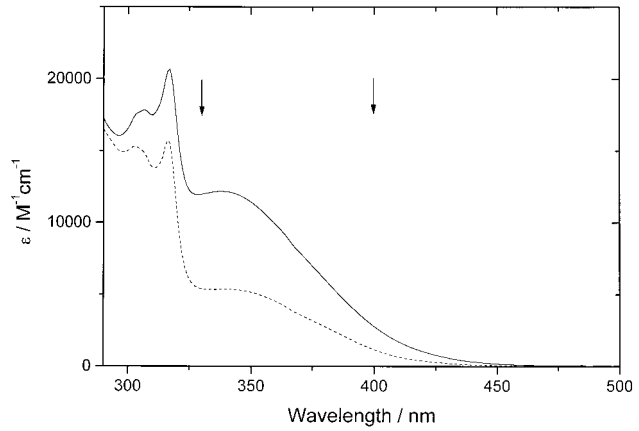

Figure 1. Absorption spectra of $[Re(MQ^+)(CO)_3(dmb)]^{2+}$ (—) and $[Re(Etpy)(CO)_3(dmb)]^+$ (- - -) in CH_3CN solutions. Arrows indicate the excitation wavelengths used in kinetic experiments. Molar absorptivities at excitation wavelengths: 400 nm, 2.8×10^3 M^{-1} cm^{-1} for $[Re(MQ^+)(CO)_3(dmb)]^{2+}$, 1.4×10^3 M^{-1} cm^{-1} for $[Re(Etpy)(CO)_3(dmb)]^+$; 330 nm, 1.2×10^4 M^{-1} cm^{-1} for $[Re(MQ^+)(CO)_3(dmb)]^{2+}$, 5.8×10^3 M^{-1} cm^{-1} for $[Re(Etpy)(CO)_3(dmb)]^+$.

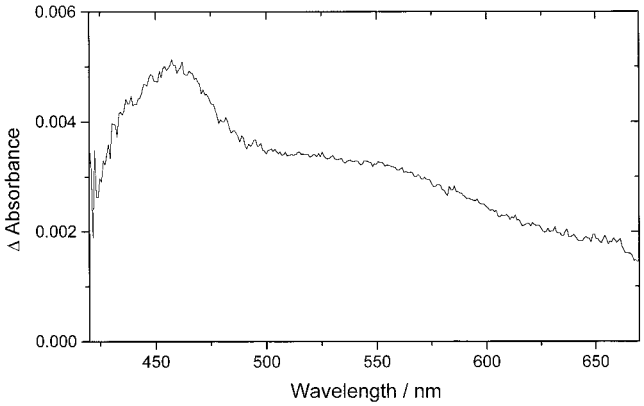

Figure 2. Picosecond time-resolved absorption spectrum of $[Re(Etpy)(CO)_3(dmb)]^+$ in CH_3CN measured at 4 ps after 400 nm excitation.

vs Fc/Fc^+ were observed in CH_3CN. In ethylene glycol, these waves are chemically only partially reversible, occurring at −1.21 and −1.73 V. (Note that the absolute values of $E_{1/2}$ in ethylene glycol are only approximate since it was not possible to measure the Fc/Fc^+ potential directly. However, this does not affect the potential difference, 0.52 V.) According to previous studies,[6−8] the first and second reduction waves were assigned to the ligand-localized $MQ^+/MQ^\bullet$ and $dmb/dmb^{\bullet-}$ redox couples, respectively. A third wave due to the $MQ^\bullet/MQ^-$ couple was found in CH_3CN at −1.98 V. Cyclic voltammograms of $[Re(MQ^+)(CO)_3(dmb)]^{2+}$ measured in CH_3CN at 273 K using a Pt electrode and a 0.1 M Bu_4NPF_6 electrolyte show a chemically nearly reversible Re^{II}/Re^{I} oxidation wave at +1.20 V and four reduction waves at −1.26, −1.76, −1.96, and −2.50 V vs Fc/Fc^+. The last wave, attributed to the $dmb^{\bullet-}/dmb^{2-}$ reduction, is chemically only partially reversible.

Picosecond Time-Resolved Spectroscopy. Shown in Figure 2 is the time-resolved absorption spectrum of $[Re(Etpy)(CO)_3(dmb)]^+$ measured in CH_3CN at 4 ps after 400 nm excitation. It displays a very weak absorption throughout the visible spectral region with an apparent maximum at about 460 nm, which arises from an onset of the bleached ground-state absorption. Neither the band shape nor the intensity change over the time interval examined, i.e., 1 ns. The absorbance monitored at 460, 555, and 660 nm is also constant. Since no spectral evolution occurs, the absorption is attributed to the long-lived Re → dmb MLCT

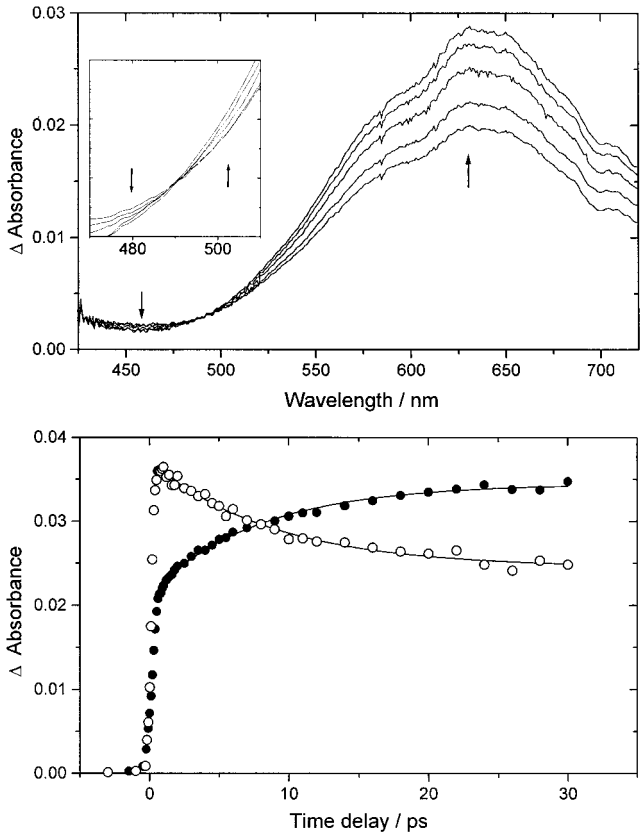

Figure 3. Top: Picosecond time-resolved absorption spectra of $[Re(MQ^+)(CO)_3(dmb)]^{2+}$ in CH_3CN measured at 2, 4, 8, 16, and 30 ps after 400 nm excitation. The spectra evolve in the direction of the arrows. The inset shows details of the isosbestic behavior in the 470−510 nm region. Bottom: Kinetic profiles of the transient absorbance measured at 460 nm (○, decay) and 660 nm (●, rise).

excited state, hereinafter denoted MLCT(dmb), whose presence was established by earlier emission studies[8,16] and by transient resonance Raman spectroscopy.[7] Moreover, the time-resolved spectrum of $[Re(Etpy)(CO)_3(dmb)]^+$ is very similar to that of the MLCT(dmb) state of $[Re(Br)(CO)_3(dmb)]$ obtained at 50 ps and 10 ns.[17−19]

Time-resolved spectra of $[Re(MQ^+)(CO)_3(dmb)]^{2+}$ measured in CH_3CN and ethylene glycol following 400 nm excitation are shown in Figures 3 and 4, respectively. They display a very weak absorption between 425 and 475 nm and an intense, structured band at 630 nm. A comparison with the 4 ps spectrum of $[Re(Etpy)(CO)_3(dmb)]^+$ (Figure 2) allows us to assign the 425−475 nm absorption to the MLCT(dmb) excited state $[Re^{II}(MQ^+)(CO)_3(dmb^{\bullet-})]^{2+}$. The 630 nm band is attributed to the MLCT(MQ^+) excited state $[Re^{II}(MQ^\bullet)(CO)_3(dmb)]^{2+}$. This assignment is based on the following observations: (i) The MLCT(MQ^+) excited state of a very similar complex, $[Re(MQ^+)(CO)_3(bpy)]^{2+}$, has been well characterized in the nanosecond time domain by transient resonance Raman[7] and UV−vis absorption[5] spectroscopy. The characteristic broad, intense absorption band found[5] in the nanosecond time-resolved spectrum of $[Re(MQ^+)(CO)_3(bpy)]^{2+}$ and assigned to the MLCT(MQ^+) excited state corresponds well to the 630 nm absorption band observed herein in the picosecond spectra of $[Re(MQ^+)$-

(16) Caspar, J. V.; Meyer, T. J. *J. Phys. Chem.* **1983**, *87*, 952.
(17) Rossenaar, B. D.; Stufkens, D. J.; Vlček, A., Jr. *Inorg. Chim. Acta* **1996**, *247*, 247.
(18) Rossenaar, B. D.; Stufkens, D. J.; Vlček, A., Jr. *Inorg. Chem.* **1996**, *35*, 2902.
(19) Kalyanasundaram, K. *J. Chem. Soc., Faraday Trans. 2* **1986**, *82*, 2401.

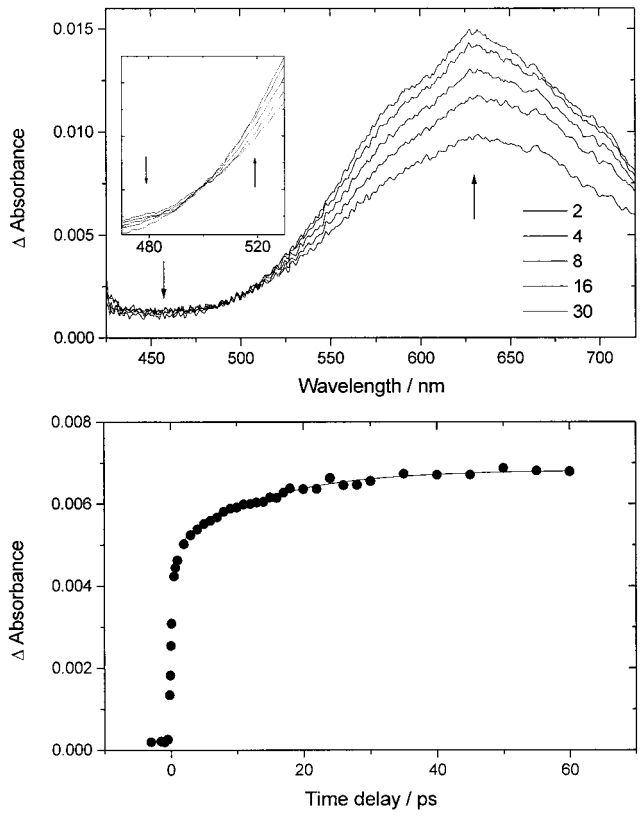

Figure 4. Top: Picosecond time-resolved absorption spectra of [Re(MQ$^+$)(CO)$_3$(dmb)]$^{2+}$ in ethylene glycol measured at 2, 4, 8, 16, and 30 ps after 400 nm excitation. The spectra evolve in the direction of the arrows. The inset shows details of the isosbestic behavior in the 470−530 nm region. Bottom: Kinetic profile of the transient absorbance measured at 660 nm (●, rise).

(CO)$_3$(dmb)]$^{2+}$. This close similarity of the absorption spectra allows us to assign the 630 nm transient to the MLCT(MQ$^+$) state, formulated as [Re^{II}(MQ$^•$)(CO)$_3$(dmb)]$^{2+}$. (ii) Moreover, the spectrum of the reduced complex [Re(MQ$^•$)(CO)$_3$(dmb)]$^+$, which contains the same MQ$^•$ chromophore as the MLCT(MQ$^+$) excited state, shows an intense, broad band at ca. 600 nm with shoulders at about 563 and 703 nm.[20] The close similarity between this band and the 630 nm absorption band of the photogenerated transient further supports the assignment of the latter to a species containing the MQ$^•$ chromophore, that is, the MLCT(MQ$^+$) excited state [Re^{II}(MQ$^•$)(CO)$_3$(dmb)]$^{2+}$. (It should be noted that a complete identity between the spectra of the reduced and MLCT excited complexes cannot be expected, since the MQ$^•$ ligand is coordinated to a metal atom in different oxidation states, Re^{II} and Re^{I}, respectively.)

The picosecond time-resolved spectra display a prominent temporal evolution during the first 30 ps after excitation (Figures 3 and 4, top): The 425−475 nm absorption decreases with a concurrent growth of the 630 nm band. An isosbestic point at about 490 and 500 nm occurs in CH_3CN and ethylene glycol, respectively. This spectral time evolution clearly demonstrates that the MLCT(dmb) excited state undergoes a direct, clean conversion into the MLCT(MQ$^+$) state, presumably by a dmb$^{•-}$ → MQ$^+$ interligand electron transfer. The kinetics of this process were studied in detail by measuring absorbance time−profiles at selected probe wavelengths; see Figures 3 and 4, bottom. Measurements performed at 460 nm show that the 425−475 nm transient due to MLCT(dmb) is formed virtually instantaneously. It is fully developed within the instrument time resolution, i.e., <600 fs. It then decays with kinetics that fit the equation $\Delta A = A_0 + A_1\exp(-t/\tau_d)$, yielding a MLCT(dmb) lifetime, τ_d, of 8.8 ± 0.8 ps in CH_3CN. The behavior of the 630 nm transient was probed at 640 and 660 nm. It follows that a significant part of the 630 nm transient is also formed "instantaneously", already within the instrument time resolution. This is manifested by the initial sharp rise of the transient absorbance and by the significant presence of the 630 nm band in the earliest time-resolved spectrum recorded at 2 ps. A slower rise then ensues. The kinetics fit the equation $\Delta A = A_0' + A_1'(1 - \exp(-t/\tau_r))$, with a rise time, τ_r, of 8.3 ± 0.4 ps in CH_3CN and 14.0 ± 1.6 ps in ethylene glycol. The $A_0'/(A_0' + A_1')$ ratio corresponds to the relative amount of the transient formed within the first 600 fs. The rise time of the MLCT(MQ$^+$) state is, within experimental uncertainty, identical to the lifetime of the MLCT(dmb) state. This observation provides further evidence for the direct MLCT(dmb) → MLCT(MQ$^+$) conversion. The values of 8.3 ± 0.4 ps in CH_3CN and 14.0 ± 1.6 ps in ethylene glycol thus correspond to the reaction lifetime of the interligand electron transfer. The respective rate constants are 1.20×10^{11} and 7.14×10^{10} s^{-1}.

The relative amount of the 630 nm transient instantaneously formed within the instrument time resolution was determined as ca. 61% after excitation at 400 nm. A very close value of ca. 52% was obtained upon 330 nm excitation. It follows that about half of the total population of the MLCT(MQ$^+$) state ultimately formed arises from an ultrafast process other than the interligand electron transfer. This initial population of the MLCT(MQ$^+$) state is prepared directly by optical excitation of [Re(MQ$^+$)(CO)$_3$(dmb)]$^{2+}$, since irradiation into the absorption band excites both the Re → dmb and Re → MQ$^+$ MLCT transitions, as was demonstrated[7] by resonance Raman spectra of ground-state [Re(MQ$^+$)(CO)$_3$(bpy)]$^{2+}$. Moreover, a comparison between UV−vis absorption spectra of [Re(Etpy)(CO)$_3$(dmb)]$^+$ and [Re(MQ$^+$)(CO)$_3$(dmb)]$^{2+}$ in Figure 1 shows that the bands due to the Re → dmb and Re → MQ$^+$ MLCT transitions of the latter complex are virtually superimposed. The molar absorptivity due the Re → MQ$^+$ MLCT transition can be estimated as a difference between the molar absorptivities of the [Re(MQ$^+$)(CO)$_3$(dmb)]$^{2+}$ and [Re(Etpy)(CO)$_3$(dmb)]$^+$ complexes. It follows (Figure 1) that the intensities of the Re → dmb and Re → MQ$^+$ MLCT transitions in [Re(Etpy)(CO)$_3$(dmb)]$^+$ are nearly identical at both excitation wavelengths. Hence, optical excitation is expected to produce approximately identical populations of the MLCT(dmb) and MLCT(MQ$^+$) excited states.

The processes observed can be summarized:

$$[Re^{I}(MQ^+)(CO)_3(dmb)]^{2+} \xrightarrow{h\nu} [Re^{II}(MQ^+)(CO)_3(dmb^{•-})]^{2+} + [Re^{II}(MQ^{•})(CO)_3(dmb)]^{2+} \quad (1)$$

$$[Re^{II}(MQ^+)(CO)_3(dmb^{•-})]^{2+} \xrightarrow{et} [Re^{II}(MQ^{•})(CO)_3(dmb)]^{2+} \quad (2)$$

The MLCT(MQ$^+$) state then decays to the ground state:

$$[Re^{II}(MQ^{•})(CO)_3(dmb)]^{2+} \xrightarrow{k_b} [Re^{I}(MQ^+)(CO)_3(dmb)]^{2+} \quad (3)$$

with a lifetime determined earlier[8] as 44 ns in 1,2-dichloroethane and <4 ns in CH_3CN. Time profiles of the absorbance at 660

(20) Berger, S.; Klein, A.; Kaim, W.; Fiedler, J. *Inorg. Chem.* **1998**, *37*, 5664.

or 640 nm, measured herein, show a decrease by 20−25% over the 200 ps to 1 ns interval examined in both CH_3CN and ethylene glycol. This would correspond to a lifetime of about 670 ps for both solvents.

The absorption spectra of the MLCT(MQ^+) state measured at 30 ps in either solvent exhibit a vibrational structure. Its magnitude cannot be determined accurately, but it is in the range of $MQ^\bullet$ intraligand vibrations, 1000−1800 cm^{-1}. Spectra measured in CH_3CN show a well-developed structure already at 2 ps, and the band shape does not change over the 2−30 ps time interval. On the other hand, the earliest spectra measured in ethylene glycol at 2 or 4 ps are largely smooth, while the vibrational structure becomes fully apparent at 16 or 30 ps; compare Figures 3 and 4. The delayed appearance of the vibrational structure in ethylene glycol suggests that the MLCT-(MQ^+) state is initially formed vibrationally hot and/or in a nonequilibrium solvent configuration.

Mechanism of the $dmb^{\bullet-} \rightarrow MQ^+$ Interligand Electron Transfer. The excited-state dynamics of $[Re(MQ^+)(CO)_3(dmb)]^{2+}$ is summarized by eqs 1−3 and Scheme 1. According to the X-ray structure[6] of $[Re(MQ^+)(CO)_3(bpy)]^{2+}$, the MQ^+ ligand is twisted with a dihedral angle between the pyridine rings of 47°. This twisted geometry is presumably preserved in the relaxed MLCT(dmb) excited state and in both optically prepared excited states, viz., MLCT(MQ^+) and MLCT(dmb), eq 1. On the other hand, the $MQ^\bullet$ ligand in the relaxed MLCT-(MQ^+) state, shown in Scheme 1, has a planar quinoidal structure, evidenced by the typical intense visible absorption band in the red spectral region and by a large, +61 cm^{-1}, shift of the frequency of the inter-ring stretching CC vibration relative to the ground-state value.[7] The pronounced structural changes accompanying the $dmb^{\bullet-} \rightarrow MQ^+$ electron transfer imply large inner-sphere reorganization energy λ_i. To estimate the overall reorganization energy pertinent to the interligand electron transfer (reaction 2), the data for $bpy^{\bullet-} \rightarrow PQ^{2+}$ electron transfer in complexes with covalently linked bpy-PQ^{2+} ligands can be used since the structural changes of PQ^{2+} and MQ^+ on reduction are similar (PQ^{2+} = *N*,*N*′-dimethyl-4,4′-bipyridinium dication). Estimates based on bpy/$bpy^{\bullet-}$ and $PQ^{2+}/PQ^{\bullet+}$ self-exchange rates[21] and on the experimental $\Delta G°$ vs k_{et} dependence[22] consistently yielded a λ value of 0.5 eV. Considering that, contrary to PQ^{2+}, the MQ^+ ligand has only one electron-acceptor pyridinium ring which is farther away from the bpy ligand, the actual λ value for reaction 2 is supposed to be somewhat larger, most probably in the 0.6−0.8 eV range. This conclusion is corroborated by the fact that the spectroscopic Re → dmb and Re → MQ^+ MLCT transitions occur at about the same energy despite the 0.5 V difference between the reduction potentials of MQ^+ and dmb. This observation implies that the reorganization energy connected with the $dmb^{\bullet-} \rightarrow MQ^+$ electron transfer should exceed 0.5 eV. It is likely that a large part of the reorganization energy comes from internal modes of the MQ^+ ligand. This view is supported by the fact that the reorganization energy pertinent to the $bpy^{\bullet-} \rightarrow PTZ^+$ back electron transfer in $[Re^I(py\text{-}PTZ^+)(CO)_3(bpy^{\bullet-})]^+$, whose PTZ redox center does not undergo a significant structural change, was estimated[23,24] as only 0.37−0.43 eV; py-PTZ = 10-(4-picolyl)phenothiazine.

The driving force, $-\Delta G°$, of the $dmb^{\bullet-} \rightarrow MQ^+$ electron transfer (reaction 2) is taken simply as the difference in the MQ^+ and dmb redox potentials, 0.49 and 0.52 eV in CH_3CN and ethylene glycol, respectively. The electrostatic contribution was neglected.[22] Since $-\Delta G° \leq \lambda$, reaction 2 occurs in the Marcus normal region.

The interligand $dmb^{\bullet-} \rightarrow MQ^+$ electron transfer in CH_3CN follows the usual nonadiabatic behavior. Application of the classical eq 4 yields an electronic coupling, V_{el}, of 2.60 × 10^{-3}

$$k_{NA} = \frac{2\pi {V_{el}}^2}{\hbar(4\pi\lambda k_B T)^{1/2}} \exp\left[-\frac{(\Delta G° + \lambda)^2}{4\lambda k_B T}\right] \qquad (4)$$

or 4.56 × 10^{-3} eV, that is, 21 or 37 cm^{-1}, for the reorganization energy λ = 0.6 or 0.8 eV, respectively. The adiabaticity parameter H_A was estimated[25,26] using eq 5 with an average

$$H_A = \pi {V_{el}}^2 \tau_S / \hbar\lambda \qquad (5)$$

value of the CH_3CN relaxation time, τ_S, of 260 fs.[27] The values obtained, 0.014−0.032 for λ = 0.6−0.8 eV, are much less than 1, confirming the assumed nonadiabaticity.

The situation is, however, different in ethylene glycol. On the basis of a slightly larger (by 0.03 eV) driving force and ca. 1.06-fold smaller ($1/D_{op} - 1/D_S$) solvent dielectric function, the nonadiabatic electron-transfer rate in ethylene glycol is expected to be comparable or slightly faster than in CH_3CN. Instead, the interligand electron transfer is about 1.7 times slower, $(14\ ps)^{-1}$, as compared with $(8.3\ ps)^{-1}$ in CH_3CN. Using an average solvent relaxation time of 15 ps,[28,29] and the V_{el} values determined in CH_3CN, eq 5 gives H_A values of 0.807 and 1.861 for λ = 0.6 and 0.8 eV, respectively. This shows that the interligand electron transfer occurs at the boundary between adiabatic and nonadiabatic regimes. Hence, eq 4 is no longer applicable. The maximum rate can be estimated[25,26] as $k = k_{NA}/(1+H_A)$. Taking the k_{NA} value of $(8.3\ ps)^{-1}$ measured in CH_3CN, the rate constant in ethylene glycol is estimated as k_{et} = $(15.0\ ps)^{-1}$ or $(23.7\ ps)^{-1}$, for λ = 0.6 or 0.8 eV, respectively. (For a barrierless electron transfer, i.e., λ = 0.52 eV, we get k_{et} = $(14.01\ ps)^{-1}$ as the fastest possible rate.) The experimental value of $(14.0\ ps)^{-1}$ is reasonably close or slightly faster than the rate constants calculated for mixed adiabatic−nonadiabatic behavior. It follows that, in ethylene glycol, the rate of the $dmb^{\bullet-} \rightarrow MQ^+$ electron transfer becomes largely controlled by the slow solvent relaxation dynamics. However, the rather fast rate constant observed indicates a contribution from high-frequency promoting nuclear vibration(s). The torsional movement of the two pyridine rings of the MQ^+ ligand seems to be the most likely candidate.[6,7] The pyridinium ring rotation is expected to be slower in ethylene glycol due to its much higher viscosity as compared with CH_3CN, 17.87 and 0.345 cp at 25 °C, respectively.

Only a few other cases of interligand electron transfer have been reported in the literature, all of them being much slower than the $dmb^{\bullet-} \rightarrow MQ^+$ process studied herein. For example,

(21) Mecklenburg, S. L.; Peek, B. M.; Schoonover, J. R.; McCafferty, D. G.; Wall, C. G.; Erickson, B. W.; Meyer, T. J. *J. Am. Chem. Soc.* **1993**, *115*, 5479.
(22) Yonemoto, E. H.; Saupe, G. B.; Schmehl, R. H.; Hubig, S. M.; Riley, R. L.; Iverson, B. L.; Mallouk, T. E. *J. Am. Chem. Soc.* **1994**, *116*, 4786.
(23) Chen, P.; Duesing, R.; Graff, D. K.; Meyer, T. J. *J. Phys. Chem.* **1991**, *95*, 5850.
(24) Katz, N. E.; Mecklenburg, S. L.; Graff, D. K.; Chen, P.; Meyer, T. J. *J. Phys. Chem.* **1994**, *98*, 8959.
(25) Jortner, J.; Bixon, M. *J. Chem. Phys.* **1988**, *88*, 167.
(26) Heitele, H. *Angew. Chem., Int. Ed. Engl.* **1993**, *32*, 359.
(27) Pogge, J. L.; Kelley, D. F. *Chem. Phys. Lett.* **1995**, *238*, 16.
(28) Cushing, J. P.; Butoi, C.; Kelley, D. F. *J. Phys. Chem. A* **1997**, *101*, 7222.
(29) Gardecki, J.; Horng, M. L.; Papazyan, A.; Maroncelli, M. *J. Mol. Liq.* **1995**, *65/66*, 49.

(4,4′-X_2-bpy$^{\bullet-}$) → PTZ$^{\bullet+}$ back electron transfer in excited [Re^{I}(py-PTZ)$(CO)_3$(4,4′-X_2-bpy)]$^+$ occurs[23] with rate constants in the range $(1-7) \times 10^7$ s^{-1}, depending on X. The electronic coupling term was estimated as 44 cm^{-1}. The slow rate is clearly due to the inverted character of this process, for which the driving force values, $-\Delta G°$, range from 1.18 to 1.93 eV.[23] The interligand electron transfer in the MLCT excited state of [Os(bpy)$_3$]$^{2+}$ is somewhat different from the present case since it corresponds to an electron hopping between equivalent ligands, bpy$^{\bullet-}$ → bpy.[27,28] Hence, it occurs with a zero driving force. The nonadiabatic rate constant and electronic coupling of (τ = 130 ps)$^{-1}$ and 15 cm^{-1}, respectively, were determined in CH_3CN.

Finally, it is interesting to note that the dmb$^{\bullet-}$ → MQ$^+$ electron transfer in [Re(MQ$^+$)$(CO)_3$(dmb)]$^{2+}$, in which the electronic coupling is mediated by the Re metal atom, is faster than photodriven electron-transfer reactions in systems where an electron acceptor is linked to the 4-position of a 2,2′-bipyridine (bpy) ligand by an organic bridging group. For example, a rate constant of 5.9×10^{10} s^{-1} (τ = 17 ps) and V_{el} = 24 cm^{-1} have been determined[22] in acetonitrile for a bpy$^{\bullet-}$ → PQ^{2+} electron transfer in a MLCT excited state of [Ru(bpy)$_2$(bpy-CH_2-PQ^{2+})]$^{4+}$. Similar reactions with longer or different linkages or other electron acceptors are even slower, usually in the range 10^7-10^8 s^{-1}, which corresponds to the nanosecond time domain. Nevertheless, MLCT excitation of some of these systems triggers spectacular photodriven electron-transfer processes. For example, an electron−hole separation across a polypeptide unit,[21] a pH-dependent electro-photoswitch,[30] a molecular "plug-in" for rapid delivery of electrons or holes to buried enzyme active units,[31] or a reversible electron transfer between an excited state of Ru(bpy)$_3^{2+}$ and the attached C_{60} group[32] were observed. By comparison, the present results on [Re(MQ$^+$)$(CO)_3$(dmb)]$^{2+}$ suggest that systems capable of excited-state electron transfer between ligands linked and held in a defined position by a metal atom can take advantage of ultrafast electron−hole separation.

Conclusions

Optical excitation of [Re(MQ$^+$)$(CO)_3$(dmb)]$^{2+}$ prepares concurrently the MLCT(dmb) and MLCT(MQ$^+$) Franck−Condon states which originate in electron excitation from a Re d(π) orbital to π* orbitals of the dmb and MQ$^+$ ligand, respectively.

The MLCT(dmb) state undergoes a picosecond dmb$^{\bullet-}$ → MQ$^+$ interligand electron transfer which produces a long-lived MLCT(MQ$^+$) state. The dmb$^{\bullet-}$ → MQ$^+$ electron transfer occurs in the Marcus normal region, apparently with only a small activation barrier. In CH_3CN, it behaves as a typical nonadiabatic process which occurs with a lifetime of 8.3 ps.

The dmb$^{\bullet-}$ → MQ$^+$ electron transfer is partly adiabatic in ethylene glycol, controlled by the solvation dynamics, perhaps with a contribution from rotation of the MQ$^+$ pyridinium ring. The reaction lifetime is 14 ps.

The MLCT(MQ$^+$) excited state relaxes to its equilibrium configuration within 2 ps in a CH_3CN solution. Relaxation appears to be slower ($\leq$16 ps) in ethylene glycol.

Acknowledgment. We thank Pavel Matousek and Tony Parker of the Rutherford Appleton Laboratories for their technical assistance and stimulating discussions. EPSRC and Queen Mary and Westfield College, University of London, are acknowledged for funding this work.

IC990770F

(30) Goulle, V.; Harriman, A.; Lehn, J.-M. *J. Chem. Soc., Chem. Commun.* **1993**, 1034.
(31) Wilker, J. J.; Dmochowski, I. J.; Dawson, J. H.; Winkler, J. R.; Gray, H. B. *Angew. Chem., Int. Ed. Engl.* **1999**, *38*, 90.
(32) Maggini, M.; Guldi, D. M.; Mondini, S.; Scorrano, G.; Paolucci, F.; Ceroni, P.; Roffia, S. *Chem. Eur. J.* **1998**, *4*, 1992.